Late autumn aerosol trace element composition and source tracking over the southern Mozambique Channel

Morgane M.G. Perron[1], Eva Bucciarelli[1], Hélène Planquette[1], Thomas Holmes[2], Saumik Samanta[3,4], Yoan Germain[5], Alakendra Roychoudhury[4], Géraldine Sarthou[1].

[1] Univ Brest, CNRS, IFREMER, IRD, LEMAR, IUEM, F-29280 Plouzané, France
[2] Australian Antarctic Program Partnership (AAPP), University of Tasmania, Battery Point, Tasmania, Australia
[3] School of Geosciences, University of the Witwatersrand, Johannesburg, South Africa
[4] Department of Earth Sciences, Stellenbosch University, Stellenbosch, South Africa
[5] IFREMER, CNRS, Univ Brest, UBS, UMR6538, Laboratoire Geo-Ocean, F-29280 Plouzané, France

Correspondence to: Morgane M. G. Perron (morgane.perron@univ-brest.fr)

Abstract.

The southern Mozambique Channel (20-30° S) receives a range of atmospheric influences, from desert dust and fire emissions through to industrial, mining and agricultural emissions, emitted from both Madagascar and southeastern Africa. Our study characterises the trace element composition of aerosols collected between the south of Madagascar and Durban, South Africa during the low dust season. Dust deposition fluxes (40-263 mg m^{-2} yr^{-1}), calculated based on Al measurement in aerosols, fell within the lower range of modelled fluxes estimates, confirming the absence of major dust or fire events during the study. While prevailing air-masses affecting our samples were modelled to originate from long-range particulate transport over the Southern Ocean, a holistic understanding of our sample composition could only be obtained when accounting for sporadic aeolian inputs from the two local landmasses. Notably, we found surprising high levels of Cr (4±2 ng m^{-3}) and Cd (0.02±0.01 ng m^{-3}) in the atmosphere over the southern Channel which could be, at least in part, attributed to emissions from mining (chromite and gold, respectively) and smelting activities (Cu, Zn and Cd co-emission) on both neighbouring landmasses. Our results emphasise the difficulty to track such specific and overlooked atmospheric sources in the absence of known atmospheric tracers. We also stress the need for multi-elemental studies and encourage the use of detailed (cluster) air-mass transport model analysis in regions dominated by the long-range atmospheric transport as complex atmospheric circulation and minor (sporadic) inputs from terrestrial air-masses may have disproportionate impact on the atmospheric composition.

1 Introduction

Atmospheric transport and deposition of trace elements play a key role in shaping marine biogeochemical cycles. In particular, iron (Fe) delivered via dust inputs can stimulate primary productivity in nutrient-limited oceanic regions, thereby modulating the marine carbon cycle (Mendez et al., 2010). Conversely, aeolian deposition can also introduce potentially toxic elements such as

cadmium (Cd), copper (Cu), lead (Pb) and zinc (Zn), emitted from urban and industrial areas, which can be deleterious for coastal marine ecosystems (Paytan et al., 2009; Thiagarajan et al., 2024; Zhou et al., 2021). Determining the relative contribution of these various sources, as well as their chemical composition is thus essential to assess their ecological impact.

The southern Mozambique Channel (defined between 20° S-30° S in this study) lies between two landmasses, namely the island of Madagascar to the east and the southeastern coast of Africa (including, South Africa and Mozambique) to the west. Both landmasses are characterised by arid to semi-arid landscapes which are increasingly prone to droughts (Barimalala et al., 2024; Mahlalela et al., 2020; Rigden et al., 2024) and wildfires (Frappier-Brinton and Lehman, 2022; Richardson et al., 2022). The dry season runs from May to October and corresponds to the most favourable period for dust entrainment into the atmosphere and long-range transport towards open ocean areas (Bhattachan et al., 2012; Ginoux et al., 2012).

Earth system models and satellite observations consistently identify the Namib Desert, the Etosha basin in Namibia, the Kalahari Desert in Botswana as well as local ephemeral rivers (Bhattachan et al., 2015) as major dust sources in Southern Africa. Seasonally, these sources contribute significantly to dust deposition across sub-tropical (25° S-40° S) latitudes of the southwest Indian Ocean (Gili et al., 2022; Jickells et al., 2005; Li et al., 2008a). In addition, during the dry season, savannah fires in southern Africa emit large plumes of nutrient-rich smoke, forming a “river of smoke” that can extend eastwards across the Mozambique Channel and even reach western Australia (Ranaivombola et al., 2025). Recently, southern Africa iron-rich dust has been linked to the formation of unusually large phytoplankton blooms in the southern Mozambique Channel south of Madagascar (Gittings et al. 2024). More locally, aeolian transport from Madagascar has also been demonstrated to carry smoke over the Mozambique Channel during the dry season (Kumar et al., 2014).

From the 21st century on, intensification of land use, including agriculture, mining, transport and urbanization, has resulted in the doubling of dust emissions from southern Africa and Madagascar Island (Hooper and Marx, 2018). In addition, to sustain the energy sectors, southern African countries are highly dependent on coal, the combustion of which contributes massive quantities of airborne particulates (Mirzania et al., 2023). Many of such thermal power plant sources, located on the east coast of South Africa, showed a four to five folds rise in particulate matter emissions over the last decade owing to the increased demand of power generation (Morosele and Langerman, 2020; Zerizghi et al., 2022). Similarly, both southern African countries and Madagascar have also recently experienced a steep increase in vehicle numbers, enhancing the vehicular and road emissions (Department of Transport, 2017; Iimi, 2023).

These anthropogenic activities emit not only nutrients but also toxic trace metals. Their finer particle size and emission processes can result in greater solubility upon deposition, making them potentially more bio-accessible (or more toxic) to micro-organisms than mineral dust (Sholkovitz et al., 2009). Mining and industrial hotspots, in the Highveld region of South Africa and near the cities of Richards Bay and Durban (South Africa) and Maputo (Mozambique) further contribute to the atmospheric burden of trace metals in the region.

Despite the diversity and intensity of surrounding natural and anthropogenic aeolian sources, no study to date has characterized the chemical composition of aerosols over the southern Mozambique Channel. Here, we present the first analysis of the atmospheric composition of trace elements, including

aluminium (Al), cadmium (Cd), chromium (Cr), copper (Cu), iron (Fe), nickel (Ni), lead (Pb), titanium (Ti), vanadium (V), and zinc (Zn), based on aerosol samples collected during the late austral autumn (April-May) 2022 over the southern Mozambique Channel. Our objective is to provide an initial assessment of the chemical variability and source signatures of atmospheric inputs to this understudied marine system.

2 Materials and Methods

2.1 Aerosol collection during the RESILIENCE campaign

The RESILIENCE (fRonts, EddieS and marIne Life in the wEstern iNdian oCEan) campaign took place aboard the R/V Marion Dufresne II in the austral autumn 2022 with the aim to better understand small scale oceanic interactions between physics and biology within Mozambique Channel eddies and rings (Penven et al., 2025; Ternon et al., 2022). The cruise departed Reunion Island on the 19th of April 2022 to explore the central Mozambique Channel and sail along the southeast coast of South Africa to arrive in Durban on the 3rd of May 2022.

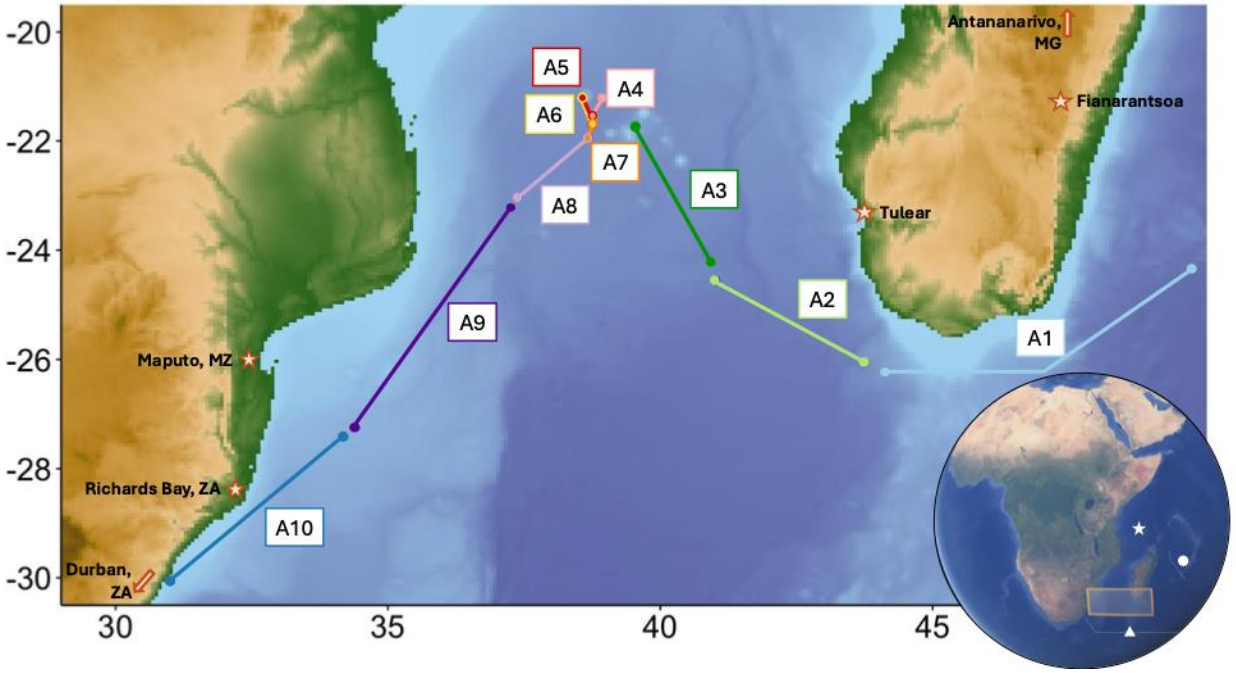

Figure 1. Location of the 10 aerosol samples, numbered A1 to A10, collected during the RESILIENCE cruise in the Southern Mozambique Channel. The inset world map indicates the location of this study (yellow rectangle) together with the location of previous field studies (symbols) reporting atmospheric trace element concentrations in the direct vicinity of our study region (triangle: Witt et al. (2006)**, circle:** Witt et al. (2010)**, star:** Chester et al. (1991)**.**

Collection of atmospheric total suspended particles was undertaken using acid-cleaned Whatman 41 filters (Cutter et al., 2017; Morton et al., 2013) and a high-volume air sampler (TE-5170, Tisch Environmental, flow rate: 1.08m^3/min). The aerosol sampler, installed on the upper viewing deck of the

ship, roughly 18 m above the sea level, enabled the collection of ten 47 mm filters simultaneously. Sampling was only undertaken when the ship was underway and under front winds (290° - 70° relative to the ship's position) to prevent contamination from the ship's smokestack. Filter holder preparation and retrieval were undertaken under a laminar flow hood placed inside a "clean bubble" laboratory in the ship. Filters were collected every 24 hours, placed in clean petri dishes using plastic tweezers and stored frozen in double sealed bags until further analysis in the land-based laboratory. Two filter blank samples, consisting of acid washed Whatman 41 which were not brought to the field, were used for blank correction as described in section 2.2. The indicative location of aerosol sampling transects is displayed in Figure 1 and the supplementary material Table S1 provides a log-sheet of all 10 aerosol samples collected, including collection dates and associated ship's coordinates.

2.2 Aerosol trace element analysis

Laboratory work was carried out in a positive pressured class 6 clean room, in an HEPA-filtered class 5 laminar flow hood wearing clean garments and nitrile gloves and following GEOTRACES 'Cookbook' procedures (Cutter et al., 2017). All chemicals used were ultra-high purity grade solutions. To assess the soluble (S_X) and total (T_X) concentrations of each target metal ("X") in aerosols, sampled filters were processed through a sequential leaching protocol modified from Perron et al. (2020). Measurements of Al, Cd, Cr, Cu, Fe, Ni, Pb, Ti, V and Zn are discussed in this study. Briefly, aerosol samples were thawed at room temperature. Each filter was placed in a centrifuge tube, soaked for 2h in 10 mL of ammonium acetate (1.4 M, pH 4.7) then centrifuged at 4200 rpm for 3 minutes. The operationally defined soluble fraction of metal in aerosols, S_X, was quantified in a 5 mL aliquot of the leachate solution following evaporation of the acetate buffer and redissolution of the residue into 0.15M nitric acid (HNO_3). The residual 5mL of leachate together with the filter were evaporated to dryness and digested using a mixture of concentrated hydrofluoric acid (14M, HF, 0.25 mL) and HNO_3 (15M, 1mL) for 12 h at 120 °C. Following another round of HNO_3 (5mL, 7M) digestion and evaporation, the refractory fraction of metal in aerosols was quantified from a 5mL HNO_3 (0.3M) aliquot. Metal concentrations in aerosol leachates were determined by Sector Field Inductively Coupled Plasma Mass Spectrometer (SF-ICP-MS, Element XR) at the Pôle Spectrométrie Ocean (Brest, France). Indium (In, 10 ng g^{-1}) was added as an internal standard in the analysed leachates to correct for potential instrumental drift during analysis. The average procedural blank was subtracted from the trace element mass measured in each leachate. The sum of measurements obtained in the two steps of the protocol defines the total fraction of trace metals in aerosols, T_X (Perron et al., 2020). The digestion and analysis of two reference materials, namely the Arizona Test Dust (<3 μm, Powder Technologies Inc®) and the Bureau of Reference plankton certified reference material (BCR-414) alongside the samples provided satisfactory recovery for all trace metals presented in this study (see supplementary Table S2). Blank contributions to the sample measured concentrations were calculated for each leaching step and are displayed in the supplementary Table S3. The refractory fraction of metal in aerosol was, for some samples, below blank levels. These measurements, for which T_X only corresponds to S_X concentration in aerosols (see Table S4), are flagged in red in Tables and are excluded from subsequent calculations.

Concentrations of metals in aerosols are expressed in nanogram of metal "X" per cubic meter of air filtered (ng m^{-3}). Aerosol fractional solubility is calculated as the ratio of soluble-to-total metal concentration (S_X/T_X) in a sample expressed as a percentage.

2.3 Dust deposition flux estimate

Aluminium content measured in the collected aerosols was used to estimate lithogenic (dust) deposition flux (F_{Dust}) in our study region.

Dust deposition was estimated assuming a prevailing crustal origin of Al and using the relative abundance of the metal, $[Al]_{UCC}$, in the upper continental crust (UCC) according to McLennan (2001). Based on assumptions made in previous studies (Baker et al., 2016; Marsay et al., 2022), a constant deposition velocity (V_d) of 1.2 cm s^{-1} was used to calculate F_{Dust} following Eq. (1):

$$FDust = \frac{\mathrm{TAl\ x}\ Vd}{[\mathrm{Al}]UCC} \quad (1)$$

where T_{Al} is the total Al concentration measured in aerosols, and $[Al]_{UCC}$=8.04%$_{w/w}$ (McLennan, 2001). As particle dry deposition velocity is sensitive to the particle size, the relative humidity, and wind speed, this parameter cannot be accurately calculated for each sampling period investigated. Hence, we acknowledge that uncertainty is associated with the use of a constant deposition velocity which was previously estimated to range by a factor of 2-3 (Duce et al., 1991; Marsay et al., 2022).

Due to Al showing 100% solubility in the two lowest trace element mass loading samples A2 and A7 (suggesting significant influence from anthropogenic emissions), these two samples were excluded from the determination of F_{Dust} in our study.

2.4 Tracking the source of metal in aerosols

2.4.1 Air-mass back-trajectories

Air-mass back-trajectories (AMBT) were calculated for each aerosol sample mid-sampling location-to assess potential atmospheric source influence. The HYSPLIT model (Air Resources Laboratory, NOAA, Stein et al. (2015)) was run using R packages "Splitr" (Iannone, 2016) and "openair" (Carslaw and Ropkins, 2012) and Global Forecast System (GFS 0.25°x0.25°) meteorological data. AMBT were calculated 7 days back and at a height of 10m above the sea level. Cluster analysis was used to assess the proportion of major air-masses arriving at 3 key locations in our study region. Trajectories were run every 3 hours over the duration of the voyage at each of the 3 locations for cluster analysis. This analysis enabled to model the influence of less prevailing air-masses of terrestrial origin, which can have disproportionate influence on the particulate loading of marine aerosol samples and their elemental composition.

2.4.2 Enrichment factors

Enrichment factor (EF) is a common tool used to estimate the relative contribution of lithogenic versus anthropogenic source contained for each aerosol metal investigated. EFs were calculated as the ratio of

total metal "X"-to-Al concentration measured in aerosols compared to the same ratio in the upper continental crust (UCC), following Eq. (2):

$$EF(X) = \frac{\frac{TX}{TAl}aerosol}{\frac{TX}{TAl}UCC} \quad (2)$$

Aluminium crustal content (Al, 8.04%$_{w/w}$, McLennan, 2001) was chosen as a reference in this study due to its reported prevailing lithogenic origin.

A threshold value of 10 was chosen, above which metal content in aerosols is deemed "enriched" by anthropogenic inputs (Shelley et al., 2015). Such threshold must be sufficiently high to account for natural variability across dust sources worldwide and natural fractionation processes occurring during the production, emission and transport of aerosols (Hird et al., 2024; Reimann and de Caritat, 2005). A minor and insignificant contribution of anthropogenic emissions can never be completely ruled out as it can be one of many factors resulting in the increase in one element's EF over the expected crustal value of 1.

2.4.3 Statistical analysis

Pearson's correlation test was performed to test for linear relationship between the total atmospheric concentration of paired trace elements. Supplementary Figure S3 summarizes the correlation factor calculated between each pair of elements as well as their degree of significance (p-value). In our study, Pearson's r correlation factors were defined as very strong when ranging 0.8-1.0 (Strzelec et al., 2020), with a significant correlation set for p-value <0.01.

3. Results

3.1. Prevailing atmospheric transport during the RESILIENCE campaign

Typical single back-trajectory analysis of prevailing air-masses arriving at 10m altitude at the mid-sampling time and location of each sample collected during the RESILIENCE campaign are presented in the supplementary Figure S1. Such single trajectory analysis often highlighted a prevailing air-mass origin from long-range transport over the Southern Ocean, obscuring potential inputs from the two major landmasses present in our study region.

Since model observations suggest a decrease in atmospheric loading at lower latitude (<25° S) in our study region (Flamant et al., 2022; Gili et al., 2022; Jickells et al., 2005; Li et al., 2008a; Neff and Bertler, 2015), we divided our samples into three groups according to their locations (north vs south of 25° S and proximity to the two landmasses). Additional cluster analysis (Figure 2) was computed for the 2 groups of samples in order to account for the influence from less dominant yet higher loading terrestrial air-mass.

Group I and Group III consisted of aerosol samples collected south of 25° S, with the former sample group being collected at proximity to Madagascar (A1-A2, Figure 2a and 2b) and the latter, at proximity

to southern Africa (A9-A10, Figure 2e and 2f). While Group I showed an influence from coastal air-masses originating from Madagascar (represented by the green, red and blue clusters in the Figure 2a and 2b), which accounted for up to 69% of the total incoming air-masses, Group III seemed to receive no influence from the island at all (Figure 2e and 2f).

Group II included samples A3-A8, collected at the centre of the Channel, north to 25° S, within a small sampling perimeter. Group II was characterised by a prevailing atmospheric influence from long-range transport of westerly winds across the Southern Ocean (accounting for up to 86% of the incoming air-masses as represented by the red, orange, purple and green clusters in Figure 2c and 2d). Sporadic terrestrial inputs from inland Madagascar Island were also observed in Group II aerosols, contributing 14% of the total incoming air-masses (blue cluster on the Figure 2c and 2d).

A more detailed characterisation of individual air-mass trajectories composing each cluster (Figure 2b, 2d, 2f) also emphasised additional influence of coastal Madagascar air-masses on Group I aerosols (represented by the red and orange clusters) which could be overlooked when solely accounting for the coarse cluster analysis outputs (Figure 2a, 2c, 2d). Similarly, in the detailed cluster analysis (Figure 2b, 2d, 2f), atmospheric inputs from southern Africa cannot be ruled out in any aerosol group.

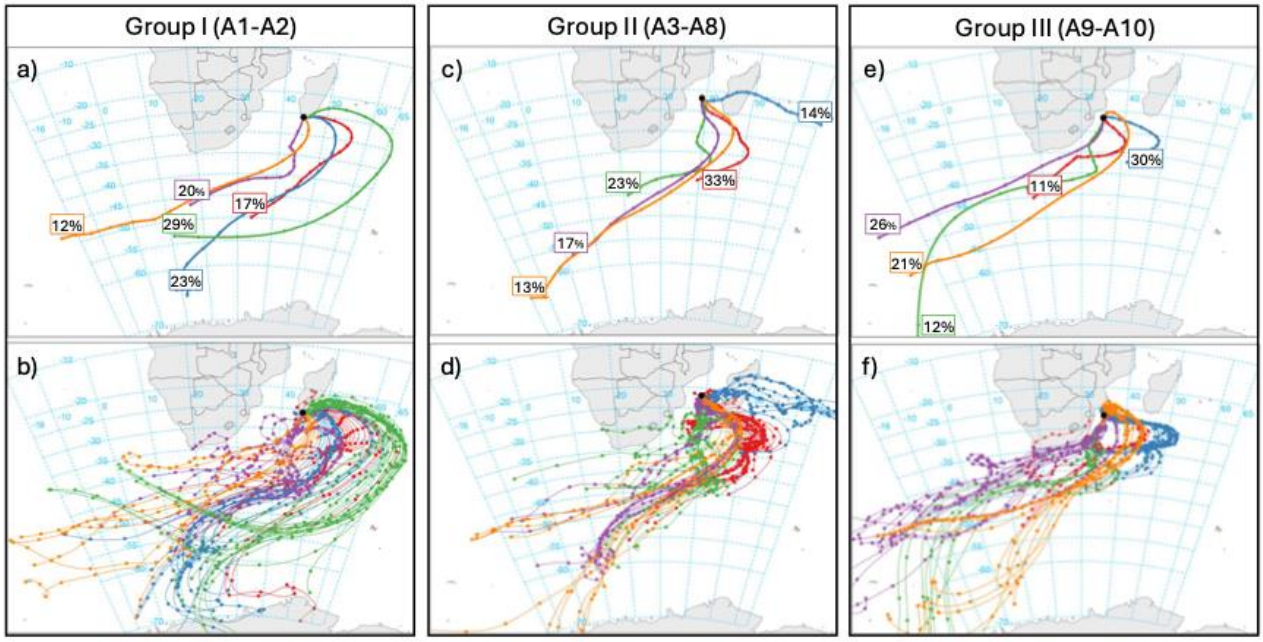

Figure 2. Seven day back-trajectory cluster analysis for the 5 prevailing air-masses arriving at 10m height at the middle location of each aerosol sample Group. Panels a), c) and e) represent the "coarse" cluster analysis including the contribution of each air-mass to the global atmospheric transport while panels b), d) and f) represent a "detailed" analysis including each air-mass trajectory and its associated cluster (colour code).

3.2. Total aeolian trace element loading over the southern Mozambique Channel

Trace element concentrations measured in individual aerosols collected in our study and total trace element mass loading data, defined as the sum of all 10 target element concentrations are reported in Table 1. The trace element total mass loading in aerosols ranged from 5.0 to 87 ng m^{-3}, with decreasing

metal contents in samples in the following order: A6>A8>A3>A9>A1>A4>A5>A10>A7>A2.
Interestingly, the trace element total mass loading measured in aerosols in our study showed a high spatial variability with no hotspot for aeolian dust deposition identified and a seemingly random distribution of high and low total mass loading across the sampling region, regardless of the sample clusters defined above (aerosol sample Groups I, II and III).
Amongst the target metals, 99% of the trace element total mass loading in our samples was comprised of Al, Cr, Cu, Fe, Ti, and Zn. These elements are subsequently referred to as "major" trace elements as opposed to "minor" trace elements, which contributed less than remaining 1% of the total metal loading in aerosols (i.e., Cd, Ni, Pb, and V).

Table 1. Total concentration of "major" (Al, Cr, Cu, Fe, Zn, and Ti) and "minor" (Cd, Ni, Pb, and V) trace elements measured in aerosol samples (A1-A10) over the southern Mozambique Channel. Median and median absolute deviation (MAD) values are indicated in the last column. Values indicated in red correspond to soluble trace metal concentrations when the refractory metal fraction was below procedural blank value and LQ represents soluble trace metal concentrations which are below the analytical limit of quantification (defined as 10*standard deviation of the analytical blank). The sum of all 10 target element concentrations is displayed as the trace element total mass loading (TE loading).

	A1	A2	A3	A4	A5	A6	A7	A8	A9	A10	Median± MAD
Major trace elements, ng m^{-3}											
Al	21.6	0.2	35.8	11.5	8.5	55.9	3.0	54.6	22.1	9.2	16±11
Cr	0.1	4.3	5.1	3.8	5.9	0.5	3.5	0.4	0.1	5.0	4±2
Cu	1.4	0.2	0.8	0.3	0.3	0.8	0.2	1.0	1.6	0.04	0.5±0.4
Fe	10.0	LQ	3.6	2.1	0.8	9.9	0.8	7.5	8.6	1.1	3±2
Ti	0.3	LQ	3.4	0.7	0.9	7.9	0.3	3.1	4.3	LQ	1±1
Zn	3.1	0.2	8.5	6.4	0.5	11.8	0.8	15.4	2.8	0.2	3±3
Minor trace elements, pg m^{-3}											
Cd	21.3	2.4	141.8	55.0	13.4	172.3	8.1	233.7	4.6	9.7	17±14
Ni	60.9	3.8	102.5	90.6	20.5	199.8	13.5	210.2	58.3	14.8	60±44
Pb	34.2	3.0	54.8	22.6	3.5	70.3	7.0	83.3	38.2	1.8	28±25
V	19.9	LQ	12.1	3.6	6.2	27.2	3.7	21.9	20.2	3.4	9±7
TE loading, ng m^{-3}	36.7	5.0	57.5	25.0	17.0	87.3	8.7	82.5	39.6	15.6	

Trace element concentrations quantified in RESILIENCE aerosol samples ranged across four orders of magnitude, from a few picograms to tens of nanograms per cubic meter of air. Amongst major trace elements, the median concentration of Al (16±11 ng m^{-3}) was at least 4 times greater than that of other major elements. Median concentrations of Cr (4±2 ng m^{-3}) were slightly higher than that of Fe (3±2 ng m^{-3}) and Zn (3±3 ng m^{-3}) while smaller concentrations were found for Ti (1±1 ng m^{-3}) and Cu (0.5±0.4 ng m^{-3}) across the range of samples collected over the southern Mozambique Channel. Amongst minor trace elements, Ni was the most abundant element (median: 60±44 pg m^{-3}), followed by Pb (28±25 pg m^{-3}), Cd (17±14 pg m^{-3}), V (9±7 pg m^{-3}).

Samples A2 and A7 stood out due to their overall low trace element content. In these aerosols, a number of analysed trace elements were only found in a soluble form (except for Cr, Cu and Ni in A2 and for Cr, Cu, Fe, Ti and Pb in A7) and the total trace element mass loadings were lower than that of other aerosol samples. Soluble trace element contribution to individual aerosol samples is displayed in the supplementary Table S4.

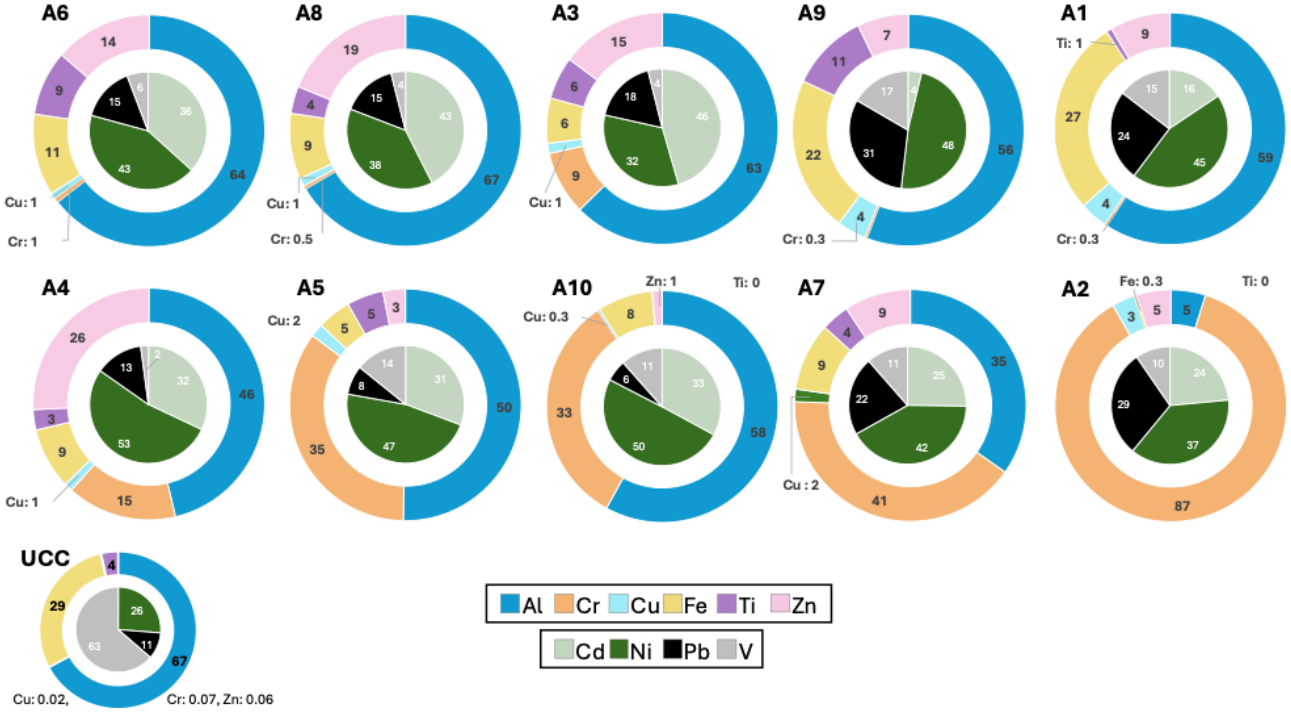

Figure 3. Relative proportion (%) of total trace elements measured in aerosols (A1-A10) over the southern Mozambique Channel. The outer (inner) circle represents major (minor) trace elements composing over 99% (less than 1%) of the total trace element mass loading in individual samples. Samples are ordered according to decreasing total metal mass loading (A6>Ax>A2). The relative composition of the average UCC (McLennan, 2001) **when accounting for the same metals is shown for comparison.**

Figure 3 offers a visual representation of the relative proportion of major and minor total trace elements measured in each aerosol sample collected over the Mozambique Channel. As a major trace element in this study, Al constituted over half of the total trace element loading (46 - 66%) in most aerosol samples collected except for A7 (35%) and A2 (5%). Higher Al abundance was found in samples with the highest total metal loading (A8>A6>A3). Variable Fe and Ti content were found across aerosol samples with generally low relative Fe abundance compared to expected crustal average (UCC), except for A1 and A9. Contrastingly, high abundances were found for Cr, Cu and Zn, from 1 to 3 orders of magnitude higher than the average UCC. In particular, low total trace elements loading samples (A2, A7, A10 and A5) displayed extremely high Cr content, composing 33% up to 87% of the sample total trace element mass loading (Figure 3). Amongst the minor elements, high relative abundances in Cd and Ni were found, which contributed 0.01-0.3% and 0.08-0.4% of the total trace element mass loading,

respectively. Relative Pb content (0.01-0.1% of the total trace element mass loading) in RESILIENCE aerosols was higher than in the average UCC, especially in A1, A2, A7 and A9.

3.3 Tracking sources of trace metal in aerosols from the southern Mozambique Channel

Enrichment factors were calculated to assess the contribution from non-lithogenic sources to individual trace elements measured in aerosols collected over the southern Mozambique Channel (Figure 4 and supplementary Figure S2), except for samples A2 and A7 where they could not be determined as the Al content in the refractory phase was below the detection limit.

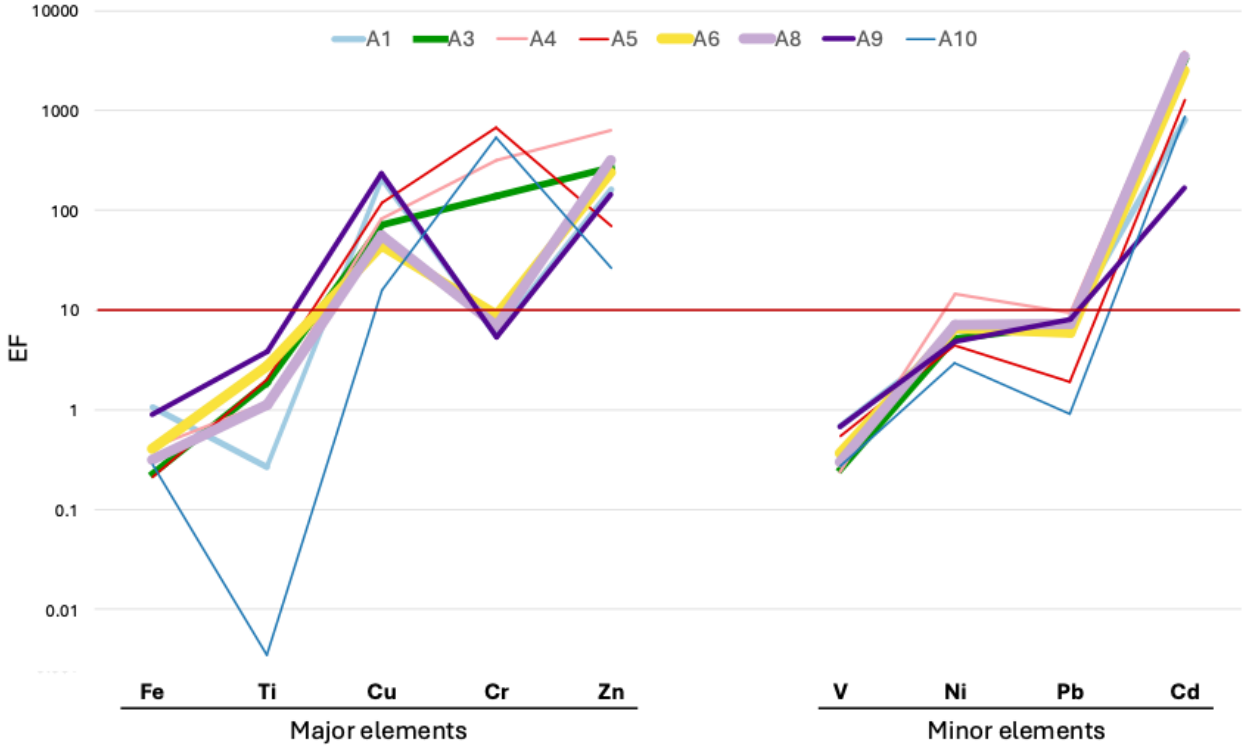

Figure 4. Enrichment factors calculated for each trace element measured in individual aerosol samples collected over the southern Mozambique Channel. The thickness of the line is proportional to the total metal loading in aerosols. The horizontal red line indicates the significant enrichment threshold value of 10 used in this study.

Amongst major elements, EFs close to 1 were found for Fe (median: 0.4) which indicated a prevailing lithogenic origin for Fe in all our aerosol samples (Figure 4). More variable EFs were calculated for Ti (median: 1.9); although values below the threshold of 10 also indicated a crustal origin for Ti in aerosols across the southern Mozambique Channel. Enrichment factors between 45 and 630 were found for Cu (median: 72) and Zn (median: 239), suggesting a significant and likely prevailing anthropogenic origin of Cu and Zn in all aerosols collected in our study, except for A10. For these two elements, however, aerosol sample A10 was characterised by much lower EF values of 16 and 26, highlighting a different or less pronounced (yet prevailing) anthropogenic influence on this sample. Contrasting enrichment was obtained for Cr (median: 138), with EF values lower than 10 calculated for high total

trace element mass loading samples (A1, A6, A8, and A9) and severe enrichment ranging 138 - 672 found in low trace element total mass loading samples (A4, A5, and A10) as well as in A3 (Figure 4). This indicates that, while natural sources dominate the Cr content in high total trace element loading samples, with no or small (insignificant) anthropogenic inputs suggested, human-derived Cr emissions are likely to predominate the Cr content in low total trace element loading samples.

Amongst minor elements, V, Ni and Pb showed EFs lower than 10, with median values of 0.4, 5.2 and 7.2, respectively (Figure 4). This indicated a prevailing crustal origin for the three metals in most aerosol samples (Reimann and de Caritat, 2005). While minor contribution from anthropogenic sources cannot be completely ruled out in the case of Ni and Pb, we consider this input insignificant with respect to the crustal contribution. Sample A4 represents one exception for which Ni enrichment exceed the threshold of 10 (EF_{Ni}=14), highlighting non-negligible inputs from anthropogenic sources in this sample. Extremely high enrichments were found for Cd (median: 2529) in all samples, with a particularly high median EF_{Cd} value of 3248 calculated for samples of Group II (A3-A8), collected north of 25° S in the centre of the Channel when compared to Group I (A1) and Group III samples (A9 and A10) which showed a median EF_{Cd} of 809.

4. Discussion

4.1 Dust deposition fluxes

The range of annual dust deposition flux calculated during the RESILIENCE cruise (40-263 mg m^{-2} yr^{-1}) falls within the low end of F_{Dust} reported by Earth System Models (ESM) (0 - 788 mg m^{-2} yr^{-1}) in the same 20° S-30° S area of the southern Mozambique Channel (Table 2). While ESM account for a yearly average F_{Dust}, our lower estimate is consistent with our study taking place at the beginning of the dry season (April-May), before the main dust and fire events which commonly occur from May to October on both Madagascar Island and the southern African continent (Bhattachan et al., 2012; Ginoux et al., 2012). While we observe a large variability in our F_{Dust} estimates, the consistency between our values and the mean annual dust deposition fluxes reported by ESM in the 20° S-30° S region of the southern Mozambique Channel could imply either 1) a limited year-to-year variability in dust deposition over the southern Mozambique Channel or 2) a poor constraint on F_{Dust} estimates by ESM due to a paucity of data. These global models vary in spatial and temporal resolution and use different satellite and ground-based observations to validate their outputs which result in a large range of dust deposition fluxes reported by different modelling studies (references in Table 2). For example, Wagener et al. (2008) used a global model output forced to fit the data obtained from two oceanographic campaigns, including around the Kerguelen Island plateau. A result from using limited observational data points to force the model seem to be an underestimate of atmospheric dust deposition at proximity from the emission sources on land. Additional field observations such those provided in our study and the use of new high-resolution satellite observation would help refining model outputs in this drastically under sampled study region where small-scale emission sources may prevail.

Table 2. Median and median absolute deviation of the dust deposition fluxes ($F_{Dust\ (Al)}$, mg m^{-2} yr^{-1}) calculated based on Al concentrations measured in RESILIENCE aerosols (southern Mozambique Channel), compared to fluxes reported by models in the southern Mozambique Channel region. Sample A2 and A7 were excluded from F_{Dust} calculation due to negligible lithogenic inputs in these samples.

Latitude	**Our study** $F_{Dust\ (Al)}$	[a]Jickells et al. (2005)	[b]Li et al. (2008)	[c]Wagener et al. (2008)	[d]Xu and Weber (2021)	[e]Westberry et al. (2023)
20°-25°S	**169±95**	0-200	158-236	2-18	30-100	∼183
>25°S	**101±2**	0-500	158-788	4-(36)*	100-316	91-(273)*

[a](Jickells et al., 2005), [b](Li et al., 2008b), [c](Wagener et al., 2008), [d](Xu and Weber, 2021) [e](Westberry et al., 2023)
*Values reported south of 30°S.

Our field-based mean F_{Dust} estimates are consistent with southern Africa being a smaller dust source to the ocean south of 20° S (Kok et al., 2021; Li et al., 2008a), compared to other provinces downwind of Australian dust sources (328 mg m^{-2} yr^{-1}; Hird et al., 2024) or that off the coast of South America (200 - 1200 mg m^{-2} yr^{-1}; Menzel Barraqueta et al., 2019). Model outputs displayed in Table 2 emphasise the south-eastwards transport of dust sources from the border junction of Namibia, Botswana and South Africa, across the African continent and into the southern Indian Ocean. Such atmospheric dust path is suggested to mostly reach latitudes south of 25° S or 30° S as depicted by high average F_{Dust} of 550 mg m^{-2} yr^{-1} reported in March during a seagoing campaign along the 32° S parallel between 30 and 40° E (Grand et al., 2015). Studies also report a decreasing influence (of a factor 2-3) of southern African dust sources as we move north of 25°S into the southern Mozambique Channel (Flamant et al., 2022; Gili et al., 2022; Jickells et al., 2005; Li et al., 2008a; Neff and Bertler, 2015; Piketh et al., 2002). Higher F_{Dust} estimates south of 25° S were not observed in our study where, on the contrary, 1.7 times increase in the mean F_{Dust} in Group II aerosol samples (Table 2) further emphasises the absence of the southern Africa dust outflow signature at the time of our study. According to HYSPLIT AMBT analysis, the prevailing atmospheric transport influencing our samples originated from the transport of westerly air-masses over the Southern Ocean, with sporadic passage over Madagascar Island and/or southern Africa that would provide most of the particulate loading in our samples. It is possible that, outside the local dust season (May-October), the south-eastwards transport of dust from major southern African sources may be absent or restricted to latitudes higher than 30° S and therefore cannot be considered as a source of dust to the Mozambique Channel. Our results corroborate findings by Freiman and Piketh (2002) that, despite 27% of the southern Africa atmospheric circulation reaches the Indian Ocean during the austral autumn, this air-mass is largely transported to the south of our study region (Freiman and Piketh, 2003). This conclusion highlights the important role of seasonality when comparing field-based measurements of dust fluxes to yearly average model estimates.

4.2 Tracking potential sources of trace elements in aerosols

AMBT analysis suggested a few recent (<7 days) inputs of terrestrial air-masses (from South Africa and/or Madagascar Island) to the southern Mozambique Channel atmospheric loading. The trace

element composition in our aerosols was tentatively used to identify specific local sources to the atmosphere coming from both neighbouring landmasses.

Table 3. Comparison of the average total trace element concentration (pmol m^{-3}) measured in all aerosols collected over the southern Mozambique Channel (this study) with existing ship-board aerosol trace element measurements in the surrounding region (locations shown in Figure 1).

	southern Mozambique Channel, this study	[a]Southern Indian (open) Ocean	[b]Tropical (open) Indian Ocean	[c]North of Reunion Island	[d]offshore Durban (coast)
season	April (early dry)	November (wet)	May (dry)	November (wet)	March (wet)
site	-25° S, 38° E	-30° S, 65° E	-8° S, 45° E	-15° S, 60° E	-32° S, 32° E
Al	822±753	772	815	1200	300 - 3600
Cu	10±9	68	3	30	20 - 75
Cr	55±44	9	3	7	
Fe	80±73	484	286	200	1500
Ti	44±54	39			
Zn	76±82	29	6	100	200
Cd	0.6±0.8	0.1	0.05	0.09	0.2
Ni	1±1	9	2	10	18 - 53
Pb	0.2±0.1	0.9	1	3	1 - 6
V	0.2±0.2	1	1	0.8	

[a](Ge et al., 2024), [b](Chester et al., 1991), [c](Witt et al., 2010), [d](Witt et al., 2006).

Overall, average atmospheric trace element concentrations measured in this study were similar (Al, Cu, and Ti) or lower (Fe, Ni, Pb and V) than data reported for marine air-masses over the southern Indian Ocean (Table 3, Chester et al., 1991; Ge et al., 2024). This finding reinforced our AMBT analysis showing a predominant influence from long-range atmospheric transport of westerly winds from across the Southern Ocean (Figure 2). However, sporadic inputs of lithogenic Al, Fe, Ni, Pb, Ti and V (EF<10, Figure 4) and anthropogenic Cu (EF_{Cu}=72, Figure 4) emissions from Madagascar and southern Africa cannot be ruled out given the proximity of both landmasses and the extensive and increasing anthropogenic activity they hold (including copper mining and smelting activity in South Africa and Zambia, Makgetla et al., 2019; Nex and Kinnaird, 2019; Sikamo, 2016). Indeed, the more detailed analysis of air-mass back trajectory transport shows, for all 3 sample groups, instances (at least one air-mass) of air-mass crossing the southern African continent then travelling over the ocean before reaching our sampling position. Such a diluted atmospheric signal observed in our study is consistent with the southern Africa atmospheric recirculation pathway previously highlighted by Freiman and Piketh (2002). Higher concentrations of anthropogenic Zn (EF_{Zn}=239, Figure 4) in our samples resembled concentrations reported downwind of anthropogenic emission sources in the southwestern Indian Ocean (Witt et al., 2006, 2010). Major sources of anthropogenic Zn to the atmosphere include coal

combustion, non-ferrous metal smelting and non-exhaust traffic emissions (Schleicher and Weiss, 2023; Wei et al., 2025). While no specific source could be pinpointed in our study, a large extent of so-called "coalfields" in the eastern and northern regions of South Africa (Hancox and Götz, 2014; Nundze et al., 2024) could be a source of Zn to the southern Mozambique Channel north of 25° S (Group II aerosols), where Zn enrichment is overall 3 times higher than in Group I and Group III samples (except for sample A5). Solid coal combustion is also widely used for cooking and heating, in a vast majority of Malagasy households (Dasgupta et al., 2013) as well as in South Africa townships (Balmer, 2007), although the magnitude of emissions linked to such practises remains unknown. Another source of Zn to the north of our study region could originate from metal smelting activities. Unlike Group I and III aerosol samples, a very strong and significant ($p<0.01$) correlation between Zn, Cd and Cu was found in our Group II samples (Figure S3) similar to previously reported near smelter facilities (Kasongo et al., 2024; Taylor et al., 2010). In addition, industrial combustion of coal was previously associated with Pb-containing easily transported fine particles while smelters tend to release coarse particle-bound Pb. The latter emissions are easier to mitigate at the source and less likely to undergo long-range aeolian transport (Zhang et al., 2024). In our study, small concentrations and insignificant enrichments ($EF<10$) of Pb in aerosols collected across the southern Mozambique Channel tend to support the role of smelter emissions as a source of atmospheric Zn, Cu and Cd rather than coal combustion emissions. Our results are in line with a modelling study by Ito and Miyakawa (2023) showing that emissions from metal production (smelting) is a major, and often overlooked, source of labile trace elements to the atmosphere over the Mozambique Channel, especially in fall when dust and pyrogenic sources are low. Most trace elements measured in Group II aerosols showed very strong and significant (p-value <0.01) correlation to Al, except for Cr and Ti (supplementary Figure S3). Such a widespread correlation between lithogenic and anthropogenic elements highlights the complex atmospheric influence in our study region as depicted in Figure 2. In aerosols collected south of 25° S (sample Groups I and III), less significant correlations were found between trace elements investigated (Figure S3).

4.3 A remaining challenge: fingerprinting mining emissions in aerosols

Amongst all trace elements measured in this study, atmospheric Cr and Cd measurements in aerosols collected over the southern Mozambique Channel stood out, with concentrations 6-18 times and 3-12 times higher than that previously reported in the surrounding region (Table 3), respectively. Such elevated metal loadings were likely associated with anthropogenic emissions as indicated by high median enrichment factors (EF_{Cr}=138 and EF_{Cd}=3248, Figure 4) and suggested the prevalence of local anthropogenic aeolian sources of Cr and Cd to the southern Mozambique Channel during our study. A negative correlation between Cr and Cd in our aerosol samples (Figure S3) suggests that two distinct sources influence the atmospheric loading of these elements over the Mozambique Channel. High atmospheric loading in Cd and Cr in our samples may raise some concern as the two metals are known pollutants with acute toxicity to both humans (Csavina et al., 2012; Ericson et al., 2008) and ecosystems (Athar and Ahmad, 2002). More specifically, high soluble fractions of Cr measured in aerosol samples A7- A10 (supplementary Table S4) collected on the western part of the southern Mozambique Channel, may indicate a predominance of Cr(VI) in the atmosphere which is carcinogenic (Świetlik et al., 2011).

Widespread Cd enrichment was observed throughout our sampling region, with an average 4.6 times increase in EF_{Cd} values in Group II aerosols (A3-A8, Figure 4) compared to aerosols collected south of 25° S (sample Groups I and III). As suggested in section 4.2, Cd emissions from smelting activities have previously been linked to elevated aerosol enrichment ($EF_{Cd(/Al)}$>1000) over the Atlantic Ocean (Shelley et al., 2015). In addition, extreme Cd enrichments relative to Fe ($EF_{Cd(/Fe)}$) up to 18800 were also reported in dust samples collected around gold mine tailing storage facilities in the South African Witwatersrand Basin (Maseki et al., 2017). In our study, Cd enrichment factors relative to Fe exceeded 763 in nearly all our aerosol samples, except in A9. A further 10-fold increase in the median enrichment factor of Cd relative to Fe ($EF_{Cd/Fe}$= 7766, Table 4) was found in aerosols from Group II compared to those of Group I and Group III ($EF_{Cd/Fe}$=763, Table 4), potentially suggesting a contribution from gold mining activities in South Africa or in Madagascar to the Cd atmospheric loading in the southern Mozambique Channel to the north of 25° S. Notably, elevated Cd concentrations have also previously been reported in squids, a known bioaccumulating species, in waters around Reunion Island (to the east of our study region), although the source of Cd in that study remained unidentified (Annasawmy et al., 2022).

Concerning Cr enrichments were observed in samples containing lower total metal mass loading (A4, A5, and A10) as well as in A3 (Figures 3 and 4). Elevated atmospheric Cr(VI) concentrations were previously associated with emissions from the ferrochrome industry in the Bushveld Igneous complex, South Africa (Venter et al., 2017). However, Venter and colleagues (2017) report a co-enrichment in Cr and Fe in aerosols which we do not observe in our samples. South Africa also holds 72–80% of the world's viable chromite ore reserves (Coetzee et al., 2020). Chromite rocks mined in Madagascar (Grieco et al., 2014) and South Africa (Kleynhans et al., 2023) have typical Cr/Fe ratios of 1.5-2.9, which largely exceeds the Cr/Fe ratio of 0.0024 in the average UCC (McLennan, 2001). Similar or higher Cr/Fe ratios (>1.4) were found in our samples A3, A4, A5, A7 and A10), indicating that Cr mining emissions might be a major contributor to the aeolian Cr loading in the southern Mozambique Channel north of 25° S (A3-A8) and close to South African coastlines (A10). While chromite mines are mostly concentrated in the north of Madagascar and in the Bushveld Igneous complex in South Africa, HYSPLIT AMBT analyses associated with our samples only rarely (Madagascar) or never (Bushveld) crossed these sources (supplementary Figure 2 and Figure S1). It is possible that our ABMT analyses does not comprise all air-masses influencing our samples and that minor atmospheric inputs from high loading terrestrial air-masses remain overlooked. In addition, other unidentified source of Cr may be influencing the atmospheric loading in our study region. For example, in Richards Bay, South Africa, discharges from the industrial sector were linked to significant enrichment in Cr, and to a lesser extent in Cd and Cu in local sediment samples collected in the harbour (Izegaegbe et al., 2023). Chromium enrichment was also previously reported in airborne particulates associated with coal mines (Dubey et al., 2012), which could also be a source in our study region. On Madagascar Island, chromium contamination of soil and water streams were also reported as a result of tannery and textile wastewater (Rasoazanany et al., 2007). Overall, our results highlight the difficulty in tracking aerosol trace element source in aerosols in the absence of specific tracers.

Table 4. Total atmospheric trace element concentration ratios (g/g) used in previous studies to trace specific anthropogenic sources in aerosols and their respective values in samples collected over the southern Mozambique Channel (this study). A2 was excluded due to extreme Fe and Cr solubility (100%) in this sample, which potentially bias the ratios displayed.

Variable	Source	Reported values	A1	A3	A4	A5	A6	A7	A8	A9	A10
Cr/Fe	[a,b] Chromite mining	1.5-2.9	0.013	**1.4**	**1.8**	**7.4**	0.053	**4.3**	0.051	0.014	**4.5**
$EF_{Cd(/Fe)}$	[c] Gold mining	<18800	763	**14107**	**9291**	5990	6242	3538	**11117**	190	3084

[a](Grieco et al., 2014), b(Kleynhans et al., 2023), [c](Maseki et al., 2017)

Conclusion

The sub-equatorial region of southern Africa drastically suffers from climate change, with temperatures rising above the global average and increasing frequency of extreme weather events (e.g., droughts, floods, cyclones, fires). This region is also affected by rapid urbanization and industrialisation of lands (Scholes et al., 2015). Such a variety of natural and anthropogenic influences most likely contribute to the atmospheric composition of the region, introducing both (bio)essential and toxic elements into the atmosphere. This study provides chemical characterisation of the trace element composition in aerosols collected over the southern Mozambique Channel (20° S-30° S) during the austral autumn 2022, when dust deposition and fire occurrence are both low (Bhattachan et al., 2012; Ginoux et al., 2012). We report a complex atmospheric circulation in the region. Indeed, while 7-day single air-mass back-trajectory computed for each sample suggested a prevailing long-range transport of aerosols by westerly winds at latitudes >25° S, a full understanding of the sources influencing the trace element loading over the southern Mozambique Channel could not be achieved without accounting for less prevailing and sporadic inputs from sources on the two major landmasses of Southern Africa and Madagascar (through detailed cluster analysis). Our observation stresses the need to investigate the full complexity of atmospheric circulation (beyond single prevailing air-mass analysis) as less frequent, terrestrial air-masses can have disproportionate impact on the particulate loading (and trace element composition) of aerosols in low deposition marine region across the Southern Hemisphere. Atmospheric metal concentrations measured in our samples were similar (Al, Cu, and Ti) or smaller (Fe, Ni, Pb and V) than concentrations previously reported in marine air-masses downwind of Southern Hemisphere emission sources. This confirmed that our study occurred during the low deposition season and that concentrations presented for the above-mentioned trace elements can be considered as background (low end) aeolian concentrations. Trace elements commonly associated with crustal sources (Al, Fe, Ti) showed no significant enrichments relative to the averaged UCC (EF<10) neither did Ni, Pb, and V despite the three metals being sometimes related to human emissions in other studies. High concentrations of Zn (and elevated Cu enrichment factor) in aerosols were associated with anthropogenic emissions which could include coal combustion and smelting. Concentrations of Cd and Cr in our aerosol samples were 3 – 18 times higher than those reported in the literature near our study region and were associated with high Cr and extremely high Cd enrichments compared to the average

UCC. Further analysis of atmospheric sources using elemental ratios in individual aerosol samples suggested inputs from mining activities (chromite: Cr, gold: Cd) to the atmosphere, especially in the central Channel between 20° S-25° S and close to the southern coastline of South Africa. Our study emphasises the difficulty in tracking specific sources of atmospheric trace elements over marine regions due to the lack of defined atmospheric tracers for specific sources such as smelting and mining for example.

Author contributions

The study was conceptualised by EB, HP, AR. Funding was secured by EB and MMGP. Samples were collected by SS. Trace element analysis and data treatment were performed by MMGP, HP and YG and air-mass analysis and data interpretation were performed by TH. Data interpretation and early manuscript drafting were undertaken by MMGP, EB, HP and GS. All authors contributed to the final manuscript drafting.

Competing interests

Authors declare that they have no conflict of interest.

Acknowledgements

The RESILIENCE cruise was supported by the French National Oceanographic Fleet operated by Ifremer, by the Belmont Forum Ocean Front Change project, implemented through the French National Research Agency (ANR-20- BFOC-0006-04), by the ISblue project, Interdisciplinary graduate school for the blue planet (ANR-17-EURE-0015) and co-funded by a grant from the French government under the program “Investissements d’Avenir” embedded in France 2030, and by the French National program LEFE (Les Enveloppes Fluides et l’Environnement). Authors wish to thank S. Herbette, M. Noyon, P. Penven and J.-F. Ternon, P.I.s of the RESILIENCE MD#257 cruise (Ternon et al., 2022) and project and the crew of the R/V ‘Marion Dufresne’ (LDA, French Oceanographic Fleet) for their help and assistance.

M.M.G.P was funded by a European Marie Sklodowska-Curie Actions fellowship number GA 101064063 and by an ISblue project, Interdisciplinary graduate school for the blue planet (ANR-17-EURE-0015) and co-funded by a grant from the French government under the program "Investissements d'Avenir" embedded in France 2030.

References

Annasawmy, P., Bustamante, P., Point, D., Churlaud, C., Romanov, E. V., and Bodin, N.: Trace elements and δ15N values in micronekton of the south-western Indian Ocean, Mar. Pollut. Bull., 184, 114053, https://doi.org/10.1016/j.marpolbul.2022.114053, 2022.

Athar, R. and Ahmad, M.: Heavy Metal Toxicity: Effect on Plant Growth and Metal Uptake by Wheat, and on Free Living Azotobacter, Water Air Soil Pollut., 138, 165–180, https://doi.org/10.1023/A:1015594815016, 2002.

Baker, A. R., Landing, W. M., Bucciarelli, E., Cheize, M., Fietz, S., Hayes, C. T., Kadko, D., Morton, P. L., Rogan, N., Sarthou, G., Shelley, R. U., Shi, Z., Shiller, A., and van Hulten, M. M. P.: Trace element and isotope deposition across the air–sea interface: progress and research needs, Philosophical Transactions of the Royal Society A: Mathematical, Physical and Engineering Sciences, 374, 20160190, https://doi.org/10.1098/rsta.2016.0190, 2016.

Balmer, M.: Household coal use in an urban township in South Africa, Journal of Energy in Southern Africa, 18, 27–32, https://doi.org/10.17159/2413-3051/2007/v18i3a3382, 2007.

Barimalala, R., Wainwright, C., Kolstad, E. W., and Demissie, T. D.: The 2019–21 drought in southern Madagascar, Weather Clim. Extrem., 46, 100723, https://doi.org/10.1016/j.wace.2024.100723, 2024.

Bhattachan, A., D'Odorico, P., Baddock, M. C., Zobeck, T. M., Okin, G. S., and Cassar, N.: The Southern Kalahari: a potential new dust source in the Southern Hemisphere?, Environmental Research Letters, 7, 024001, https://doi.org/10.1088/1748-9326/7/2/024001, 2012.

Bhattachan, A., D'Odorico, P., and Okin, G. S.: Biogeochemistry of dust sources in Southern Africa, J. Arid Environ., 117, 18–27, https://doi.org/10.1016/j.jaridenv.2015.02.013, 2015.

Carslaw, D. C. and Ropkins, K.: openair — An R package for air quality data analysis, Environmental Modelling & Software, 27–28, 52–61, https://doi.org/10.1016/j.envsoft.2011.09.008, 2012.

Chester, R., Berry, A. S., and Murphy, K. J. T.: The distributions of particulate atmospheric trace metals and mineral aerosols over the Indian Ocean, Mar. Chem., 34, 261–290, https://doi.org/10.1016/0304-4203(91)90007-J, 1991.

Coetzee, J. J., Bansal, N., and Chirwa, E. M. N.: Chromium in Environment, Its Toxic Effect from Chromite-Mining and Ferrochrome Industries, and Its Possible Bioremediation, Expo. Health, 12, 51–62, https://doi.org/10.1007/s12403-018-0284-z, 2020.

Csavina, J., Field, J., Taylor, M. P., Gao, S., Landázuri, A., Betterton, E. A., and Sáez, A. E.: A review on the importance of metals and metalloids in atmospheric dust and aerosol from mining operations, Science of The Total Environment, 433, 58–73, https://doi.org/10.1016/j.scitotenv.2012.06.013, 2012.

Cutter, G. A., Casciotti, K., Croot, P., Geibert, W., Heimbürger, L.-E., Lohan, M. C., Planquette, H., and Flierdt, T. van de.: Sampling and Sample-Handling Protocols for GEOTRACES Cruises, Version 3.0, 2017.

Dasgupta, S., Martin, P., and Samad, H. A.: Addressing Household Air Pollution: A Case Study in Rural Madagascar., 2013.

Department of Transport, S. A.: Annual Report for 2016/17 Financial Year Vote 35, 2017.

Dubey, B., Pal, A. K., and Singh, G.: Trace metal composition of airborne particulate matter in the coal mining and non–mining areas of Dhanbad Region, Jharkhand, India, Atmos. Pollut. Res., 3, 238–246, https://doi.org/10.5094/APR.2012.026, 2012.

Duce, R. A., Liss, P. S., Merrill, J. T., Atlas, E. L., Buat-Menard, P., Hicks, B. B., Miller, J. M., Prospero, J. M., Arimoto, R., Church, T. M., Ellis, W., Galloway, J. N., Hansen, L., Jickells, T. D., Knap, A. H., Reinhardt, K. H., Schneider, B., Soudine, A., Tokos, J. J., Tsunogai, S., Wollast, R., and Zhou, M.: The atmospheric input of trace species to the world ocean, Global Biogeochem. Cycles, 5, 193–259, https://doi.org/10.1029/91GB01778, 1991.

Ericson, B., Hanrahan, D., and Kong, V.: The World's Worst Pollution Problems: The Top Ten of the Toxic Twenty, 2008.

Flamant, C., Gaetani, M., Chaboureau, J.-P., Chazette, P., Cuesta, J., Piketh, S. J., and Formenti, P.: Smoke in the river: an Aerosols, Radiation and Clouds in southern Africa (AEROCLO-sA) case study, Atmos. Chem. Phys., 22, 5701–5724, https://doi.org/10.5194/acp-22-5701-2022, 2022.

Frappier-Brinton, T. and Lehman, S. M.: The burning island: Spatiotemporal patterns of fire occurrence in Madagascar, PLoS One, 17, e0263313, https://doi.org/10.1371/journal.pone.0263313, 2022.

Freiman, M. T. and Piketh, S. J.: Air Transport into and out of the Industrial Highveld Region of South Africa, Journal of Applied Meteorology, 42, 994–1002, https://doi.org/10.1175/1520-0450(2003)042<0994:ATIAOO>2.0.CO;2, 2003.

Ge, Y., Guan, W., Wong, K. H., and Zhang, R.: Spatial Variability and Source Identification of Trace Elements in Aerosols From Northwest Pacific Marginal Sea, Indian Ocean and South Pacific to Antarctica, Global Biogeochem. Cycles, 38, https://doi.org/10.1029/2024GB008235, 2024.

Gili, S., Vanderstraeten, A., Chaput, A., King, J., Gaiero, D. M., Delmonte, B., Vallelonga, P., Formenti, P., Di Biagio, C., Cazanau, M., Pangui, E., Doussin, J.-F., and Mattielli, N.: South African dust contribution to the high southern latitudes and East Antarctica during interglacial stages, Commun. Earth Environ., 3, 129, https://doi.org/10.1038/s43247-022-00464-z, 2022.

Ginoux, P., Prospero, J. M., Gill, T. E., Hsu, N. C., and Zhao, M.: Global-scale attribution of anthropogenic and natural dust sources and their emission rates based on MODIS Deep Blue aerosol products, Reviews of Geophysics, 50, https://doi.org/10.1029/2012RG000388, 2012.

Grand, M. M., Measures, C. I., Hatta, M., Morton, P. L., Barrett, P., Milne, A., Resing, J. A., and Landing, W. M.: The impact of circulation and dust deposition in controlling the distributions of dissolved Fe and Al in the south Indian subtropical gyre, Mar. Chem., 176, 110–125, https://doi.org/10.1016/j.marchem.2015.08.002, 2015.

Grieco, G., Merlini, A., Pedrotti, M., Moroni, M., and Randrianja, R.: The origin of Madagascar chromitites, Ore Geol. Rev., 58, 55–67, https://doi.org/10.1016/j.oregeorev.2013.11.002, 2014.

Hancox, P. J. and Götz, A. E.: South Africa's coalfields — A 2014 perspective, Int. J. Coal Geol., 132, 170–254, https://doi.org/10.1016/j.coal.2014.06.019, 2014.

Hird, C., Perron, M. M. G., Holmes, T. M., Meyerink, S., Nielsen, C., Townsend, A. T., de Caritat, P., Strzelec, M., and Bowie, A. R.: On the use of lithogenic tracer measurements in aerosols to constrain dust deposition fluxes to the ocean southeast of Australia, Aerosol Research, 2, 315–327, https://doi.org/10.5194/ar-2-315-2024, 2024.

Hooper, J. and Marx, S.: A global doubling of dust emissions during the Anthropocene?, Glob. Planet. Change, 169, 70–91, https://doi.org/10.1016/j.gloplacha.2018.07.003, 2018.

Iannone, R.: SplitR, https://doi.org/doi.org/10.5281/zenodo.49106, 2016.

Iimi, A.: Estimating the demand for informal public transport: evidence from Antananarivo, Madagascar, Public Transport, 15, 129–168, https://doi.org/10.1007/s12469-022-00300-9, 2023.

Jickells, T. D., An, Z. S., Andersen, K. K., Baker, A. R., Bergametti, G., Brooks, N., Cao, J. J., Boyd, P. W., Duce, R. A., Hunter, K. A., Kawahata, H., Kubilay, N., laRoche, J., Liss, P. S., Mahowald, N., Prospero, J. M., Ridgwell, A. J., Tegen, I., and Torres, R.: Global Iron Connections Between Desert Dust, Ocean Biogeochemistry, and Climate, Science (1979)., 308, 67–71, https://doi.org/10.1126/science.1105959, 2005.

Kasongo, J., Alleman, L. Y., Kanda, J.-M., Kaniki, A., and Riffault, V.: Metal-bearing airborne particles from mining activities: A review on their characteristics, impacts and research perspectives, Science of The Total Environment, 951, 175426, https://doi.org/10.1016/j.scitotenv.2024.175426, 2024.

Kleynhans, E. L. J., Beukes, J. P., van Zyl, P. G., and du Preez, S. P.: Chemical beneficiation of chromite ore to improve the chromium-to-iron ratio for ferrochrome production, Miner. Eng., 201, 108196, https://doi.org/10.1016/j.mineng.2023.108196, 2023.

Kok, J. F., Adebiyi, A. A., Albani, S., Balkanski, Y., Checa-Garcia, R., Chin, M., Colarco, P. R., Hamilton, D. S., Huang, Y., Ito, A., Klose, M., Li, L., Mahowald, N. M., Miller, R. L., Obiso, V., Pérez García-Pando, C., Rocha-Lima, A., and Wan, J. S.: Contribution of the world's main dust source regions to the global cycle of desert dust, Atmos. Chem. Phys., 21, 8169–8193, https://doi.org/10.5194/acp-21-8169-2021, 2021.

Kumar, K. R., Sivakumar, V., Yin, Y., Reddy, R. R., Kang, N., Diao, Y., Adesina, A. J., and Yu, X.: Long-term (2003–2013) climatological trends and variations in aerosol optical parameters retrieved from MODIS over three stations in South Africa, Atmos. Environ., 95, 400–408, https://doi.org/10.1016/j.atmosenv.2014.07.001, 2014.

Li, F., Ginoux, P., and Ramaswamy, V.: Distribution, transport, and deposition of mineral dust in the Southern Ocean and Antarctica: Contribution of major sources, Journal of Geophysical Research: Atmospheres, 113, https://doi.org/10.1029/2007JD009190, 2008a.

Li, F., Ginoux, P., and Ramaswamy, V.: Distribution, transport, and deposition of mineral dust in the Southern Ocean and Antarctica: Contribution of major sources, Journal of Geophysical Research: Atmospheres, 113, https://doi.org/10.1029/2007JD009190, 2008b.

Mahlalela, P. T., Blamey, R. C., Hart, N. C. G., and Reason, C. J. C.: Drought in the Eastern Cape region of South Africa and trends in rainfall characteristics, Clim. Dyn., 55, 2743–2759, https://doi.org/10.1007/s00382-020-05413-0, 2020.

Mahowald, N. M., Baker, A. R., Bergametti, G., Brooks, N., Duce, R. A., Jickells, T. D., Kubilay, N., Prospero, J. M., and Tegen, I.: Atmospheric global dust cycle and iron inputs to the ocean, Global Biogeochem. Cycles, 19, https://doi.org/10.1029/2004GB002402, 2005.

Makgetla, N., Levin, S., and Mtanga, S.: Moving up the copper value chain in Southern Africa, UNU-WIDER, https://doi.org/10.35188/UNU-WIDER/2019/686-9, 2019.

Marsay, C. M., Kadko, D., Landing, W. M., and Buck, C. S.: Bulk Aerosol Trace Element Concentrations and Deposition Fluxes During the U.S. GEOTRACES GP15 Pacific Meridional Transect, Global Biogeochem. Cycles, 36, https://doi.org/10.1029/2021GB007122, 2022.

Maseki, J., Annegarn, H. J., and Spiers, G.: Health risk posed by enriched heavy metals (As, Cd, and Cr) in airborne particles from Witwatersrand gold tailings, J. South. Afr. Inst. Min. Metall., 117, 663–669, https://doi.org/10.17159/2411-9717/2017/v117n7a8, 2017.

McLennan, S. M.: Relationships between the trace element composition of sedimentary rocks and upper continental crust, Geochemistry, Geophysics, Geosystems, 2, https://doi.org/10.1029/2000GC000109, 2001.
Mendez, J., Guieu, C., and Adkins, J.: Atmospheric input of manganese and iron to the ocean: Seawater dissolution experiments with Saharan and North American dusts, Mar. Chem., 120, 34–43, https://doi.org/10.1016/j.marchem.2008.08.006, 2010.
Menzel Barraqueta, J.-L., Klar, J. K., Gledhill, M., Schlosser, C., Shelley, R., Planquette, H. F., Wenzel, B., Sarthou, G., and Achterberg, E. P.: Atmospheric deposition fluxes over the Atlantic Ocean: a GEOTRACES case study, Biogeosciences, 16, 1525–1542, https://doi.org/10.5194/bg-16-1525-2019, 2019.
Mirzania, P., Gordon, J. A., Balta-Ozkan, N., Sayan, R. C., and Marais, L.: Barriers to powering past coal: Implications for a just energy transition in South Africa, Energy Res. Soc. Sci., 101, 103122, https://doi.org/10.1016/j.erss.2023.103122, 2023.
Morosele, I. P. and Langerman, K. E.: The impacts of commissioning coal-fired power stations on air quality in South Africa: insights from ambient monitoring stations, Clean Air Journal, 30, https://doi.org/10.17159/caj/2020/30/2.8833, 2020.
Morton, P. L., Landing, W. M., Hsu, S., Milne, A., Aguilar-Islas, A. M., Baker, A. R., Bowie, A. R., Buck, C. S., Gao, Y., Gichuki, S., Hastings, M. G., Hatta, M., Johansen, A. M., Losno, R., Mead, C., Patey, M. D., Swarr, G., Vandermark, A., and Zamora, L. M.: Methods for the sampling and analysis of marine aerosols: results from the 2008 GEOTRACES aerosol intercalibration experiment, Limnol. Oceanogr. Methods, 11, 62–78, https://doi.org/10.4319/lom.2013.11.62, 2013.
Neff, P. D. and Bertler, N. A. N.: Trajectory modeling of modern dust transport to the Southern Ocean and Antarctica, Journal of Geophysical Research: Atmospheres, 120, 9303–9322, https://doi.org/10.1002/2015JD023304, 2015.
Nex, P. A. M. and Kinnaird, J. A.: Minerals and Mining in South Africa, 27–35, https://doi.org/10.1007/978-3-319-94974-1_4, 2019.
Nundze, S., Ogunlaja, A., Eastwood, K., Thwala, M., and Melariri, P.: Investigation of nanomaterial and hazardous emissions at coal-fired power stations in Mpumalanga, South Africa, S. Afr. J. Sci., 120, https://doi.org/10.17159/sajs.2024/16062, 2024.
Paytan, A., Mackey, K. R. M., Chen, Y., Lima, I. D., Doney, S. C., Mahowald, N., Labiosa, R., and Post, A. F.: Toxicity of atmospheric aerosols on marine phytoplankton, Proceedings of the National Academy of Sciences, 106, 4601–4605, https://doi.org/10.1073/pnas.0811486106, 2009.
Penven, P., Ternon, J., Noyon, M., Herbette, S., Cambon, G., Comby, C., L'Hégaret, P., Malauene, B. S., Ménesguen, C., Nehama, F., Rauntenbach, G., Rufino, Y., and Sudre, F.: Characterizing the Central Structure of a Mesoscale Eddy-Ring Dipole in the Mozambique Channel From In Situ Observations, J. Geophys. Res. Oceans, 130, https://doi.org/10.1029/2024JC021913, 2025.
Perron, M. M. G., Strzelec, M., Gault-Ringold, M., Proemse, B. C., Boyd, P. W., and Bowie, A. R.: Assessment of leaching protocols to determine the solubility of trace metals in aerosols, Talanta, 208, https://doi.org/10.1016/j.talanta.2019.120377, 2020.
Piketh, S. J., Swap, R. J., Maenhaut, W., Annegarn, H. J., and Formenti, P.: Chemical evidence of long-range atmospheric transport over southern Africa, Journal of Geophysical Research: Atmospheres, 107, https://doi.org/10.1029/2002JD002056, 2002.

Ranaivombola, M., Bègue, N., Vaz Peres, L., Fazel-Rastgar, F., Sivakumar, V., Krysztofiak, G., Berthet, G., Jegou, F., Piketh, S., and Bencherif, H.: Characterization of aerosol optical depth (AOD) anomalies in September and October 2022 over Skukuza in South Africa, Atmos. Chem. Phys., 25, 3519–3540, https://doi.org/10.5194/acp-25-3519-2025, 2025.
Rasoazanany, E. O., Andriambololona, R., Andriannarivo, R. R., and Randriamanivo, L. V.: Pollution of the environment by tannery and textile waste waters in the areas of Antananarivo, Madagascar, 15 September 2007.
Reimann, C. and de Caritat, P.: Distinguishing between natural and anthropogenic sources for elements in the environment: regional geochemical surveys versus enrichment factors, Science of The Total Environment, 337, 91–107, https://doi.org/10.1016/j.scitotenv.2004.06.011, 2005.
Richardson, D., Black, A. S., Irving, D., Matear, R. J., Monselesan, D. P., Risbey, J. S., Squire, D. T., and Tozer, C. R.: Global increase in wildfire potential from compound fire weather and drought, NPJ Clim. Atmos. Sci., 5, 23, https://doi.org/10.1038/s41612-022-00248-4, 2022.
Rigden, A., Golden, C., Chan, D., and Huybers, P.: Climate change linked to drought in Southern Madagascar, NPJ Clim. Atmos. Sci., 7, 41, https://doi.org/10.1038/s41612-024-00583-8, 2024.
Schleicher, N. J. and Weiss, D. J.: Identification of atmospheric particulate matter derived from coal and biomass burning and from non-exhaust traffic emissions using zinc isotope signatures, Environmental Pollution, 329, 121664, https://doi.org/10.1016/j.envpol.2023.121664, 2023.
Scholes, B., Scholes, M., and Lucas, M.: Climate Change: Briefings from Southern Africa, Wits University Press, https://doi.org/10.18772/22015119186, 2015.
Shelley, R. U., Morton, P. L., and Landing, W. M.: Elemental ratios and enrichment factors in aerosols from the US-GEOTRACES North Atlantic transects, Deep Sea Research Part II: Topical Studies in Oceanography, 116, 262–272, https://doi.org/10.1016/j.dsr2.2014.12.005, 2015.
Sholkovitz, E. R., Sedwick, P. N., and Church, T. M.: Influence of anthropogenic combustion emissions on the deposition of soluble aerosol iron to the ocean: Empirical estimates for island sites in the North Atlantic, Geochim. Cosmochim. Acta, 73, 3981–4003, https://doi.org/10.1016/j.gca.2009.04.029, 2009.
Sikamo, J.: Copper mining in Zambia - history and future, J. South. Afr. Inst. Min. Metall., 116, 491–496, https://doi.org/10.17159/2411-9717/2016/v116n6a1, 2016.
Stein, A. F., Draxler, R. R., Rolph, G. D., Stunder, B. J. B., Cohen, M. D., and Ngan, F.: NOAA's HYSPLIT Atmospheric Transport and Dispersion Modeling System, Bull. Am. Meteorol. Soc., 96, 2059–2077, https://doi.org/10.1175/BAMS-D-14-00110.1, 2015.
Strzelec, M., Proemse, B. C., Barmuta, L. A., Gault-Ringold, M., Desservettaz, M., Boyd, P. W., Perron, M. M. G., Schofield, R., and Bowie, A. R.: Atmospheric Trace Metal Deposition from Natural and Anthropogenic Sources in Western Australia, Atmosphere (Basel)., 11, 474, https://doi.org/10.3390/atmos11050474, 2020.
Świetlik, R., Molik, A., Molenda, M., Trojanowska, M., and Siwiec, J.: Chromium(III/VI) speciation in urban aerosol, Atmos. Environ., 45, 1364–1368, https://doi.org/10.1016/j.atmosenv.2010.12.001, 2011.
Taylor, M. P., Mackay, A. K., Hudson-Edwards, K. A., and Holz, E.: Soil Cd, Cu, Pb and Zn contaminants around Mount Isa city, Queensland, Australia: Potential sources and risks to human health, Applied Geochemistry, 25, 841–855, https://doi.org/10.1016/j.apgeochem.2010.03.003, 2010.
Ternon, J.-F., Herbette, S., Penven, P., and Noyon, M.: RESILIENCE cruise, RV Marion Dufresne, https://doi.org/10.17600/18001917, 2022.

Thiagarajan, V., Nah, T., and Xin, X.: Impacts of atmospheric particulate matter deposition on phytoplankton: A review, Science of The Total Environment, 950, 175280, https://doi.org/10.1016/j.scitotenv.2024.175280, 2024.
Wagener, T., Guieu, C., Losno, R., Bonnet, S., and Mahowald, N.: Revisiting atmospheric dust export to the Southern Hemisphere ocean: Biogeochemical implications, Global Biogeochem. Cycles, 22, https://doi.org/10.1029/2007GB002984, 2008.
Wei, T., Dong, Z., Li, F., Kang, S., and Qin, X.: Quantifying the distribution and origins of aerosol zinc across the Northern Hemisphere using stable zinc isotopes: A review, J. Hazard. Mater., 491, 137828, https://doi.org/10.1016/j.jhazmat.2025.137828, 2025.
Westberry, T. K., Behrenfeld, M. J., Shi, Y. R., Yu, H., Remer, L. A., and Bian, H.: Atmospheric nourishment of global ocean ecosystems, Science (1979)., 380, 515–519, https://doi.org/10.1126/science.abq5252, 2023.
Witt, M., Baker, A., and Jickells, T.: Atmospheric trace metals over the Atlantic and South Indian Oceans: Investigation of metal concentrations and lead isotope ratios in coastal and remote marine aerosols, Atmos. Environ., 40, 5435–5451, https://doi.org/10.1016/j.atmosenv.2006.04.041, 2006.
Witt, M. L. I., Mather, T. A., Baker, A. R., De Hoog, J. C. M., and Pyle, D. M.: Atmospheric trace metals over the south-west Indian Ocean: Total gaseous mercury, aerosol trace metal concentrations and lead isotope ratios, Mar. Chem., 121, 2–16, https://doi.org/10.1016/j.marchem.2010.02.005, 2010.
Xu, H. and Weber, T.: Ocean Dust Deposition Rates Constrained in a Data-Assimilation Model of the Marine Aluminum Cycle, Global Biogeochem. Cycles, 35, https://doi.org/10.1029/2021GB007049, 2021.
Zerizghi, T., Guo, Q., Zhao, C., and Okoli, C. P.: Sulfur, lead, and mercury characteristics in South Africa coals and emissions from the coal-fired power plants, Environ. Earth Sci., 81, 116, https://doi.org/10.1007/s12665-021-10046-5, 2022.
Zhang, J., Sun, X., Wu, Q., Deng, J., Li, Z., Wen, M., Xu, L., Gu, Y., Han, T., Feng, L., and Duan, L.: Emission characteristics of lead and particulate matter from lead and zinc smelters in China, J. Hazard. Mater., 476, 135224, https://doi.org/10.1016/j.jhazmat.2024.135224, 2024.
Zhou, W., Li, Q. P., and Wu, Z.: Coastal phytoplankton responses to atmospheric deposition during summer, Limnol. Oceanogr., 66, 1298–1315, https://doi.org/10.1002/lno.11683, 2021.